Environmental Science and Pollution Research (2019) 26:26351–26366
https://doi.org/10.1007/s11356-019-05907-3

RESEARCH ARTICLE

Microarray analysis of apoptosis gene expression in liver injury induced by chronic exposure to arsenic and high-fat diet in male mice

Heibatullah Kalantari[1] · Mohammad Javad Khodayar[1] · Najmaldin Saki[2] · Layasadat Khorsandi[3] · Ali Teymoori[4] · Hadis Alidadi[1] · Azin Samimi[1]

Received: 6 January 2019 / Accepted: 3 July 2019 / Published online: 9 July 2019

Abstract

Rapid growth in the incidence of liver disease is largely attributable to lifestyle and environmental contaminants, which are often overlooked as the leading causes of this problem. Thus, the possible contribution of arsenic (As) to high-fat diet (HFD)–induced liver damage was examined via microarray analysis. To perform this experiment, a total number of 40 healthy adult male NMRI mice (22–30 g) were used. To this end, these animals were randomly assigned to four groups of 10. Oxidative stress and histopathological parameters were also evaluated in the liver of the mice exposed to a minimally cytotoxic concentration of As (50 ppm) in drinking water while being fed with a HFD for 20 weeks. Subsequently, apoptosis gene expression profiling was utilized via real-time (RT) PCR array analysis. The results showed that As had increased the amount of HFD-induced liver damage and consequently amplified changes in oxidative stress factors, histopathological parameters, as well as apoptosis pathway genes. Investigating the expression profile of apoptosis pathway genes similarly revealed that caspase-8, as a main upstream contributor to the apoptosis pathway, might play an important role in the induction of apoptosis generated by As and HFD. Ultimately, this study highlighted that As in drinking water could increase sensitivity in mice to HFD-induced liver disease through strengthening apoptosis pathway.

Keywords Arsenic · High-fat diet · Oxidative stress · Apoptosis · Microarray analysis

Introduction

Cell population control system can be disrupted following exposure to toxicants. It is also dependent on homeostatic regulation of cell proliferation, differentiation, and apoptosis (Bashir et al. 2006). In this respect, apoptosis refers to an early, chronic, and temperate response subsequent to damage induction (Elmore 2007). Besides, chronic exposure to As is presumed to be one of the major public health challenges at present (Yu et al. 2009). It should be noted that As is known as a metalloid that is universally distributed in nature, and humans are mainly exposed to this toxicant through food and water (Hong et al. 2014). According to the report released by the World Health Organization (WHO), > 200 million people around the world are exposed to As at concentrations higher than the standard 10 μg/l permissible limit (Choudhury et al. 2016). The etiologic role of As for the liver has been similarly considered more controversial since liver has been recognized as one of the most favored organs for As toxicity and also considering that As methylation mostly occurs in the liver (Liu and Waalkes 2008). Despite evidence of the importance of As, the question arises of how As leads to various diseases. It should be noted that As-associated detrimental effects can directly inhibit complex I of mitochondrial electron transport chain and elevate levels of cytochrome P450 which will lead to high rates of reactive oxygen species (ROS) production that, in turn, favor increased rate of lipid peroxidation (Majumdar et al. 2011; Nutt et al. 2005). This boosted ROS consecutively causes a depolarization of mitochondrial

Responsible editor: Philippe Garrigues

✉ Azin Samimi
Azin.samimi831@gmail.com

[1] Department of Pharmacology and Toxicology, School of Pharmacy, Ahvaz Jundishpur University of Medical Sciences, Ahvaz, Iran

[2] Research Center of Thalassemia & Hemoglobinopathy, Health Research Institute, Ahvaz Jundishapur University of Medical Sciences, Ahvaz, Iran

[3] Cellular and Molecular Research Center, Ahvaz Jundishapur University of Medical Sciences, Ahvaz, Iran

[4] Department of Virology, School of Medicine, Ahvaz Jundishapur University of Medical Sciences, Ahvaz, Iran

membrane, a decrease in ATP levels, and loss of mitochondrial membrane permeabilization (MMP) which all initiate apoptosis (Flora et al. 2009; Santra et al. 2007). Paradoxically, As is reported to be a susceptible carcinogen as well (Martinez et al. 2011). This contrasting behavior of As is fairly concentrated and depends on cell types. Chronic- and low-concentration exposures have been also described to be responsible for carcinogenesis including skin, lung, and liver but not apoptosis whereas high concentration of As has been blamable for apoptosis in different cell types (Rehman and Naranmandura 2013; Roy et al. 2016; Singh et al. 2011). However, the universal scenario of instrumental genes and their interactions leading to amplification of apoptotic signals are yet to be completely uncovered. Most studies nowadays have focused on the adverse effects of As alone and this toxicant has not been considered as a booster along with other risk factors for diseases which may affect pathophysiological changes or disease states. In several countries characterized by high concentrations of As in drinking water, HFD-induced obesity is also prevalent. Thus, there is a potential overlap in areas of risks for As exposure and obesity (Wahlang et al. 2013). It should be noted that obesity results from a persistently positive energy balance (Kleinert et al. 2018). An increase in food availability, in particular high-energy diet, also seems to account for the development of obesity (Wang et al. 2014). So, this medical condition has become a global epidemic, contributing to the increasing burdens of cardiovascular diseases, type 2 diabetes, some types of cancer, and premature death (Jelinek et al. 2013). Although obesity and consequently its metabolic disorders caused by over-nutrition and sedentary lifestyle have turned into an epidemic worldwide, the underlying mechanisms have yet to be elucidated. Under obesity conditions, lipid storage capacity of adipocytes is exceeded, resulting in adipocyte-derived fatty acids and cytokines leaking into circulation (Guilherme et al. 2008). Harmful lipid species then accumulate in ectopic tissues such as liver and pancreas (Feldstein et al. 2004). Hepatic damage following excessive consumption of fatty foods or delivery of fatty acids in the liver also lead to suppressed hepatic ability to break down and store fat. Moreover, in obesity, insulin resistance promotes lipolysis and increases free fatty acid delivery to the liver (Ahmed 2015; Choi and Diehl 2008; Listenberger et al. 2003). In addition to fatty acids, altered secretion of adipokines (such as adiponectin) or lipokines also contribute to metabolic impairments in this tissue (Fasshauer and Bluher 2015). Under these conditions, enhanced fatty acid metabolism leads to substantial mtDNA, increases mitochondrial respiratory, produces excessive mitochondrial ROS in the liver, and consequently suppresses the transcription of key antioxidant genes which eventually result in apoptosis (Liu et al. 2005; Rector et al. 2010).

Exposure to environmental chemicals also modifies human transcriptome (Mitchell et al. 2016). Considering that transcriptomic analysis has the ability to study the change of gene expression in different organisms and plays an important role in understanding human disease, it was employed to examine the results of the present study.

It should be noted that apoptosis response is a central pathway in liver disease pathophysiology across species and caspases 8 activation, as a main upstream player in the apoptosis pathway, is necessary and sufficient to cause such cell death (Wang 2015). Likewise, As-related oxidative stress and HFD metabolism are adequate to instigate liver damage and consequently induce apoptosis (Dutta et al. 2014). The chronic hepatocellular damage attributed to oxidative stress and apoptosis (second hit) also results in hepatocellular dysfunction. Eventually, these dual insults can lead to the development of liver diseases. Thus, it was hypothesized that As could collaborate with HFD to cause liver diseases through disrupting balance in oxidative stress and making subsequent changes in apoptotic pathway genes (Fig. 1).

Materials and methods

Animals

In this experimental study, a total number of 40 healthy adult male NMRI mice (22–30 g) were provided by the Animal Research Ethics Committee of Ahvaz Jundishapur University of Medical Science (AJUMS). This study was also

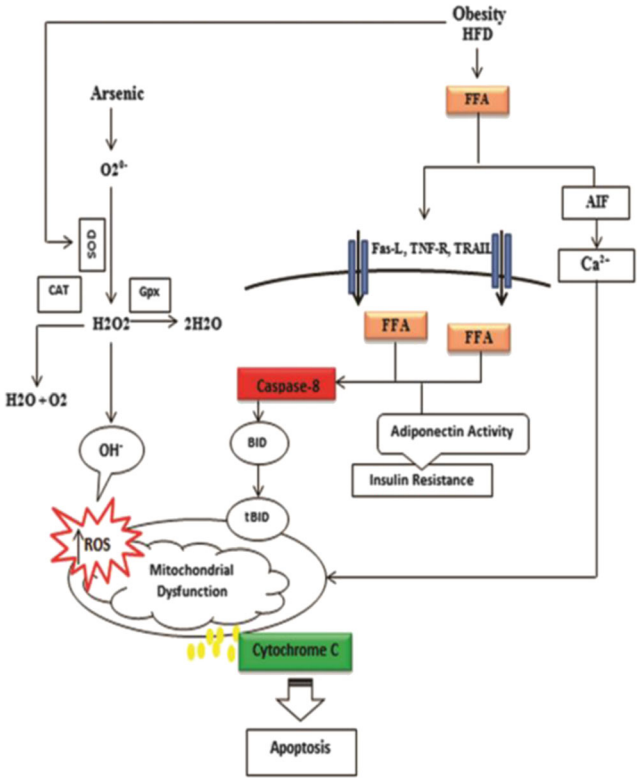

Fig. 1 Interaction of oxidative stress and apoptosis pathways in chronic exposure of arsenic and high-fat diet

fully approved by the AJUMS Animal Care Guidelines and Ethics Committee (No. IR.AJUMS.TRC9608). These animals were then housed (10 mice per cage) in polycarbonate cages under standard conditions (temperature about 20 ± 4 °C with 12/12 h light/dark cycle and 10% humidity).

Experimental design

The animals were randomly assigned to four groups of 10. The LFD group (11% fat, 16% protein, and 72.8% carbohydrate kcal/g) which was considered as the control group, the HFD group (58% fat, 16.4% protein, and 25.5% carbohydrate kcal/g), and the other two groups received the HFD and the LFD together with As (50 ppm). According to previous studies, the duration of the experimental period was considered by 20 weeks and As concentration of 50 ppm was chosen in this study (Ahangarpour et al. 2018; Zeinvand-Lorestani et al. 2018b). Water containing As was freshly prepared every 3 days to minimize oxidation of As (III) to As (V). Daily water and food consumption were then measured in all exposure groups. Body weight and fasting blood glucose (FBG) were subsequently determined every week. After 20 weeks, the mice were anesthetized with ketamine and xylazine and the whole blood was gathered. The mice were then sacrificed by decapitation and harvested liver tissue was isolated from each animal. One part of the liver was fixed in phosphate-buffered formalin (10%) for histological assessments and terminal deoxynucleotidyl transferase dUTP nick end labeling (TUNEL) staining. For the assessment of biochemical markers, one section was homogenized with chilled Tris–HCl buffer (0.1 M, pH 7.4) and stored at − 80 °C. The supernatants were then assessed for protein concentration using the Bradford protein assay (Bradford 1976). The other section was shock-frozen in liquid nitrogen and kept in − 80 °C for quantitative reverse transcription polymerase chain reaction (qRT-PCR).

MDA level assay

First, 15 g of TCA, 0.375 g of TBA, and 0.25 of N HCl were mixed. Then, 1000 μl of the mixture was blended with 500 μl of the homogenate. The obtained mixture was subsequently boiled for 15 min and centrifuged for 10 min at 3500×*g*. The absorbance was read at 532 nm using a spectrophotometer (UV-160A, Shimadzu, Japan) and the results were stated as nmol/mg protein (Buege and Aust 1978).

GSH level assay

To precipitate the homogenates, 100 ml of TCA (25%) was used and it was removed via centrifuge. Then, 2 ml of DTNB (0.5 mM) was blended with 0.1 ml of the supernatants. The absorbance of the samples was subsequently quantified at 412 nm using a spectrophotometer (UV-160A, Shimadzu, Japan) and GSH content was expressed as nmol/ mg protein (Ellman 1959).

Antioxidant enzyme (CAT, SOD, and GPx) activity assay

To measure CAT activity, 200 ml of phosphate buffer was added to 50 ml of the tissue supernatant. Then, it was mixed with 250 ml of H2O2 (0.066 M) and the decrease in OD was evaluated at 240 nm for 60s (Aebi 1984). The SOD enzyme action was also measured using Ransod unit (Randox Labs, UK). In this method, a water-soluble formazan dye was produced upon reduction with superoxide anion. The price of the diminishment with a superoxide anion was directly identified with the xanthine oxidase (XO) action and was prevented by the SOD. The inhibition activity of the SOD could be determined using a spectrophotometer at 505 nm (Elwej et al. 2016). The GPx activity was similarly specified utilizing a Ransel kit (Randox Labs., Crumlin, UK) according to Paglia and Valentine (Paglia and Valentine 1967). It should be noted that GPx catalyzes the oxidation of glutathione via cumene hydroperoxide. In the presence of glutathione reductase and NADPH, the oxidized glutathione (GSSG) is immediately converted into the reduced form with a concomitant oxidation of NADPH to $NADP^+$. The decrease in absorbance is also monitored via a spectrophotometer at 340 nm. The activities of all the enzymes are thus expressed as units per milligram protein.

TUNEL staining

The in situ Cell Death Detection kit (POD, Roche) was used for TUNEL staining. The paraffin sections were then dewaxed and incubated with proteinase K for 0.5 h at 24 °C. Afterwards, the sections were exposed to the TUNEL reaction mixture in a humidity chamber at 37 °C for 1 h. To this end, the sections were first incubated with anti-fluorescein-AP for 0.5 h at 37 °C, rinsed in deionized water, and incubated with DAB substrate (Sigma-Aldrich) for 5 min. The cells with a homogeneous dark brown nucleus were also considered to be TUNEL-positive ones (Doğanyiğit et al. 2019).

Histopathological evaluation

Paraffin sections (5 μm) were prepared and stained with hematoxylin and eosin (H&E) and trichrome for assessment the histological changes such as accumulation of RBCs, infiltration of inflammatory cells, fat deposits, and fibrosis. A total number of 6 slides per animal were evaluated. These indicators were also graded into 4 categories: normal (0), weak (1), moderate (2), or intense (3), and their averages were also taken into account. Fatty change was graded according to the

percentage of hepatocytes containing macrovesicular fat (grade 1, 0–25%; grade 2, 26–50%; grade 3, 51–75%; grade 4, 76–100%). For each slide, the mean of 6 fields was calculated. The slides were read in a "blind" fashion (Kirsch et al. 2003; Zou et al. 2006).

Evaluation of genes associated with apoptosis process via RT^2 profiler™ PCR array

In this study, apoptosis gene expression profiling through RT2 profiler PCR arrays-mouse apoptosis was utilized (Table 1). The total RNA was also isolated from 30 mg of each sample according to RNeasy Mini Kit (QIAGEN, Cat No. 74104). All the samples were then tested for RNA volume using spectrophotometer (Nano Drop 1000, Thermo Scientific, Pittsburgh, PA) at the wavelengths of 260–280 nm. Then, the cDNA was synthesized from 500 ng total RNA by RT^2 PCR array first strand kit (QIAGEN, Cat No. 330401). cDNA was also diluted by adding RNase-free water. Moreover, the PCR was carried out using a Light Cycler® 480 apparatus (Roche Applied Science).

After centrifuging RT2 SYBR Green Mastermix (10–15 s), the components of PCR mix was prepared using the values required for RT2 SYBR Green Mastermix, cDNA synthesis reaction, and RNase-free water according to the kit protocol. RT2 SYBR Green Mastermix was also centrifuged for 10–15 s, combined with cDNA synthesis components, and then RNase-free water was used for the components of PCR mix preparation based on the kit protocol. The PCR mix (25 μl) was also transferred into each well of the plate, left at ambient temperature between 15 and 25 °C for 1 min, and centrifuged at 1000*g* to remove the appeared bubbles. The kit guidelines (Roche LightCycler 480) were also followed to set the real-time cycler program. In this respect, the real-time cycler software was applied to calculate the threshold cycle (CT). The attained data were then analyzed using the $2^{-\Delta\Delta CT}$ method, indicating fold change as fold upregulation (> 1) and fold downregulation (< 1). The housekeeping genes in the present study included actin, beta (Actb), beta-2 microglobulin (B2m), glyceraldehyde-3-phosphate dehydrogenase (Gapdh), heat shock protein 90 alpha (cytosolic), and class B member 1 (Hsp90ab1). It should be noted that the expression levels of the gene of interest (GOI) and HKG genes were divided for normalization of GOI to HKG.

$$\frac{2^{-CT(GOI)}}{2^{-CT(HKG)}} = 2^{-[CT\ (GOI)-CT\ (HKG)]} = 2^{-\Delta CT}$$

Then, the normalized GOI expression in the experimental sample was divided by the normalized GOI expression in the control to calculate the fold change in gene expression:

$$\frac{2^{-\Delta CT\ (expt)}}{2^{-\Delta CT\ (ctrl)}} = 2^{-\Delta\Delta CT}$$

where ΔΔCT is equal to ΔCT (expt) − ΔCT (ctrl).

The following equation shows the complete calculation:

$$\frac{\frac{2^{-\Delta CT\ (GOI)\ expt}}{2^{-\Delta CT\ (HKG)\ expt}}}{\frac{2^{-\Delta CT\ (GOI)\ ctrl}}{2^{-\Delta CT\ (HKG)\ ctrl}}} = \frac{2^{-[CT\ (GOI)-\Delta CT\ (HKG)]\ expt}}{2^{-[CT\ (GOI)-\Delta CT\ (HKG)]\ ctrl}} = \frac{2^{-\Delta CT\ expt}}{2^{-\Delta CT\ ctrl}} = 2^{-\Delta\Delta CT}$$

The primary pathway database that we chose was KEGG because it is popular, is manually curated, has a high inner-

Table 1 Genes listed by RT2 profiler PCR arrays-mouse apoptosis

Induction of apoptosis	
Death domain receptors	Cradd, Fadd, Tnf, Tnfrsf10b (DR5)
DNA damage and repair	Cidea, Cideb, Trp53 (p53), Trp63 (Tp73l), Trp73
Extracellular apoptotic signals	Cflar (Casper), Dapk1
Other pro-apoptotic genes	Bad, Bak1, Bax, Bcl10, Bcl2l11, Bid, Bnip3, Bnip3l, Bok, Casp1 (ICE), Casp12, Casp14, Casp2, Casp3, Casp4, Casp6, Casp8 (FLICE), Cd70 (Tnfsf7), Dffa, Dffb, Diablo (Smac), Fas(Tnfrsf6), Fasl (Tnfsf6), Mapk1 (Erk2), Nod1 (Card4), Pycard (Tms1, Asc), Tnfsf10 (Trail), Trp53bp2, Traf3
Anti-apoptotic	
Akt1, Api5, Atf5, Bag1, Bag3, Bax, Bcl2, Bcl2l1 (Bcl-XL), Bcl2l10, Bcl2l2, Birc3 (cIAP1, cIAP2), Birc5, Bnip2, Bnip3, Bnip3l, Cd40lg (Tnfsf5), Cflar (Casper), Dad1, Dapk1, Fas (Tnfrsf6), Igf1r, Il10, Lhx4, Mcl1, Naip1(Birc1), Naip2, Nfkb1, Nme5, Nol3, Polb, Prdx2, Tnf, Trp63 (Tp73l), Xiap (Birc4)	
Regulation of apoptosis	
Negative regulation of apoptosis	Bag1, Bag3, Bcl10, Bcl2, Bcl2a1a, Bcl2l1, Bcl2l10, Bcl2l2, Birc2, Birc3, Bnip2, Bnip3, Bnip3l, Casp3, Cd40lg, Cflar, Cidea, Dapk1, Dffa, Fas, Mcl1, Nol3, Trp53, Trp73, Xiap
Positive regulation of apoptosis	Abl1, Akt1, Anxa5, Bad, Bak1, Bax, Bcl2l11, Bid, Bnip3, Bnip3l, Card10, Casp1, Casp14, Casp2, Casp4, Casp6, Casp8, Cd40, Cd70, Cideb, Cradd, Fadd, Fasl, Gadd45a, Ltbr, Nod1, Pycard, Tnf, Tnfrsf10b, Tnfsf10, Tnfsf12, Trp53, Trp53bp2, Traf1, Traf2, Traf3

coherence, and is academically available in a downloadable format .

Cytochrome C release assay

The level of cytochrome C in the cytosol was further assayed using a cytochrome C ELISA Kit (abcam, Cambridge, MA, USA). Moreover, a total of 50 μL of supernatant from homogenized tissue and 50 μL of antibody cocktail was also added to each well and incubated for 1 h at room temperature. Each well was then washed with 3× 350 μL 1× wash buffer PT. In this respect, 100 μL of TMB substrate was added to each well and incubated for 6 min in darkness. Afterwards, 100 μL of stop solution was added to each well and recorded at 450 nm. It should be noted that the concentration of cytochrome C was expressed as nanogram per milligram protein.

Statistical analyses

Data were presented as means ± SEM. All the results were analyzed using Graph Pad Prism (version 7.03). Statistical significance was determined using the one-way analysis of variance with the Tukey post hoc test and the non-parametric Kruskal-Wallis test. Statistical significance was set at $p < 0.05$.

Results

Body weight, water, and food intake

The results of this study demonstrated that daily water and food intake had been significantly affected by HFD and As exposure (50 ppm). The animals in all three groups drinking less water and consuming less food were also compared with the control group ($p < 0.05$, $p < 0.01$ and $p < 0.001$). The animals were found to have a significant intake of As although they had been treated with As of 50 ppm and drunk less water (Ahangarpour et al. 2018). Moreover, mice fed with HFD had received more calories and gained higher final average weight despite less food consumption ($p < 0.01$). In the HFD + As (50 ppm) group, As had also led to weight loss ($p < 0.01$) and this decline in the mice exposed to As (50 ppm) alone was not reported significant (Table 2).

FBG

It should be noted that concomitant administration of As and HFD leads to a different type 2 of diabetes, which is characterized by impaired glucose tolerance and islet's insulin secretion or content without typical symptoms of type 2 diabetes such as insulin resistance, hyperglycemia, and hyperinsulinemia. Hepatotoxicity and oxidative stress can also occur in this model of diabetes (Ahangarpour et al. 2018). Accordingly, the control group in this study showed an average FBG level of 115.65 mg/dl after 20 weeks. The HFD feeding also resulted in a statistically significant FBG (207.34 mg/dl) which was considerably different from that in the control group ($p < 0.001$). Therefore, exposure to As (50 ppm) alone and As (50 ppm) in combination with HFD showed a tendency towards increased FBG (134.37 and 133.26 mg/dl respectively) in comparison with the control group in which such differences were not statistically significant (Fig. 2).

Oxidative stress parameters

The results illustrated in Fig. 3 suggested a significant increase in lipid peroxidation following exposure to As (50 ppm) alone ($p < 0.05$) and in combination with HFD ($p < 0.001$) compared with that in the control group. Also, GSH content in all three groups was significantly lower than the control group ($p < 0.01$, $p < 0.001$) compared with that in the control group. Based on the restore results in Table 3, GPx activity in all three study groups and SOD and CAT activities in the HFD + As (50 ppm) group also decreased as compared with that in the control group ($p < 0.01$, $p < 0.001$).

Table 2 Water intake, food intake, and body weight in control group, HFD group, and As-treated groups (As 50 ppm and HFD + As 50 ppm)

	Groups			
	Control	HFD	As 50 ppm	HFD + As 50 ppm
Water intake (ml/day)	8.1 ± 0.90	6.3 ± 0.90*	4.2 ± 0.50$^{***,\#\#}$	3.9 ± 0.26$^{***,\#\#}$
Food intake (mg/day)	10.33 ± 1.23	8.40 ± 1.05	7.43 ± 1.21*	5.86 ± 0.40**
Body weight (g)	26.4 ± 2.4	30 ± 6.2**	25.2 ± 1.48	24 ± 1.58$^{**\#\#\#}$

Values represented as mean ± SEM ($n = 10$)

* Significantly different from control

$^{\#}$ Significantly different from HFD

$^{*}p < 0.05$, ** and $^{\#\#}p < 0.01$, *** and $^{\#\#\#}p < 0.001$

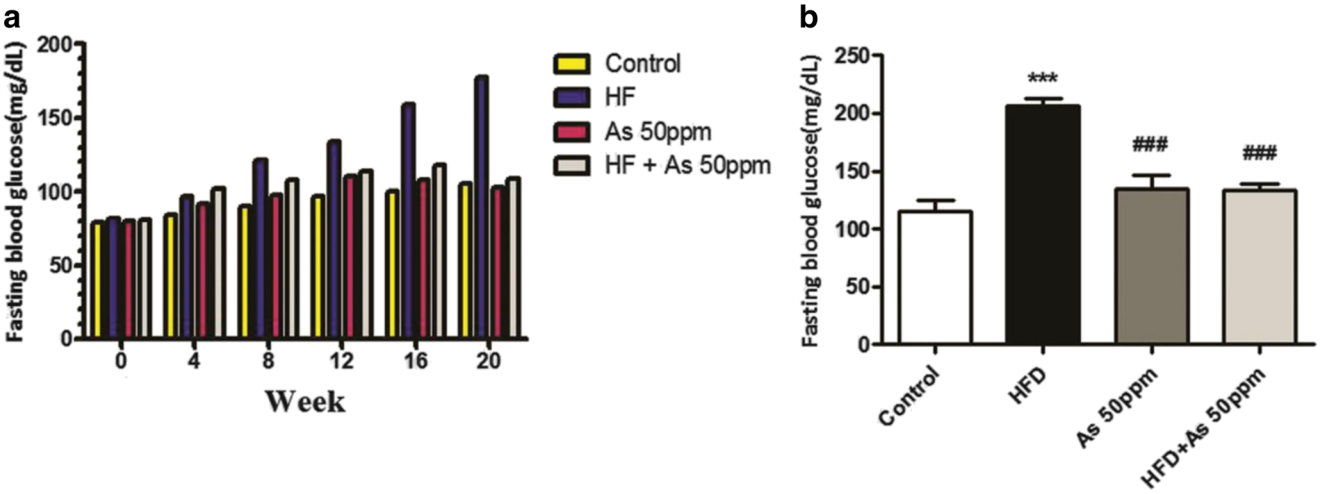

Fig. 2. Fasting blood glucose (FBG). **a** During 20 weeks and **b** at the last week in control group, HFD group, and As-treated groups (As 50 ppm and HFD + As 50 ppm). Values represented as mean ± SEM (n = 10). Asterisks mean significantly different from the control and number signs significantly different from HFD. *** and ### $p < 0.001$

TUNEL staining

As shown in Fig. 4, spontaneous apoptosis was observed in the control group. In the HFD group, the apoptotic index had also slightly increased, while the given index had significantly increased in the As group compared with that in the control group ($p < 0.05$). In the HFD + As group, numerous TUNEL-positive cells were also observed and a significant rising trend was reported in the apoptotic index compared with that in the control group ($p < 0.001$).

Histopathological analysis

The histopathological assessments of different liver sections of the experimental animals were illustrated in Figs. 5 and 6 and Table 4. A normal liver histology was observed in the control group. The liver lobular structure was also reported clear and regular and a single layer of hepatocytes had been arranged around the central vein in a radial pattern under the light microscope. Absorption of apoptotic bodies with Kupffer cells was also associated with an increase in fibrinogenic factors such as TRAIL, TNF-α, FasL, and TGF-β. So, phagocytosis of the apoptotic bodies via hepatic cells could directly stimulate fibrogenesis and apoptosis was found to be associated with increased inflammation and hepatic fibrosis (Chakraborty et al. 2012). Accordingly, accumulation of RBC, infiltration of inflammatory cells, and fat deposit significantly increased in the HFD and As groups compared with those in the control group ($p < 0.01$, $p < 0.001$). In the HFD + As group, in addition to the accumulation of RBC, infiltration of inflammatory cells and fat deposit, fibrosis was also significantly higher than that in the control group (Fig. 6), indicating a higher degree of apoptosis than that in other groups ($p < 0.001$).

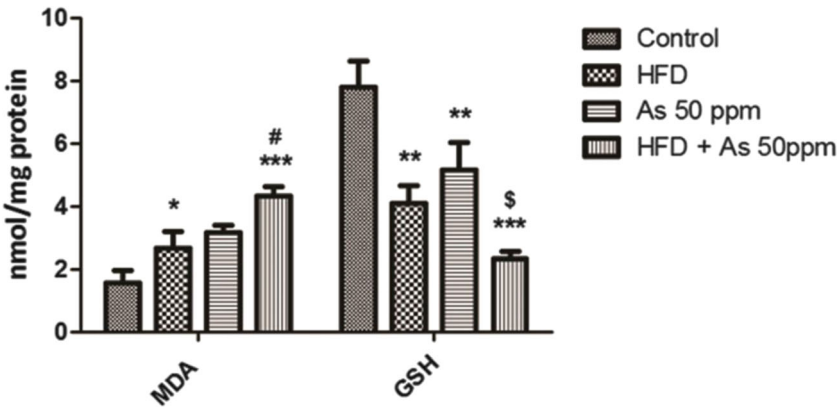

Fig. 3 Malondialdehyde (MDA) level and glutathione (GSH) level in control group, HFD group, and As-treated groups (As 50 ppm and HFD + As 50 ppm). Values represented as mean ± SEM (n = 10). Asterisks mean significantly different from control, number sign significantly different from HFD, dollar sign significantly different from As. *, # and $ $p <$ 0.05, ** $p < 0.01$, *** $p < 0.001$

Table 3 Gpx, SOD, and CAT activities in control group, HFD group, and As-treated groups (As 50 ppm and HFD + As 50 ppm)

Variables	Groups			
	Control	HFD	As 50 ppm	HFD + As 50 ppm
GPx (U/mg protein)	8 ± 0.62	5.1 ± 0.59**	5.7 ± 0.79**	2.8 ± 0.59***,#,$
SOD (U/mg protein)	3.77 ± 1.04	2.26 ± 0.65	2.49 ± 0.74	1.40 ± 0.38**
CAT (U/mg protein)	57.58 ± 10.57	38.26 ± 5.40	44.24 ± 7.22	23.14 ± 3.77**

Values represented as mean ± SEM (n = 10)

* Significantly different from control

Significantly different from HFD

$ Significantly different from As

and $ $p < 0.05$, ** $p < 0.01$, *** $p < 0.001$

Transcriptomic analysis of apoptosis gene expression in control, HFD, As, and HFD + As-treated groups

The expressions of apoptosis pathway and genes in the control group, the HFD group, and the As-treated groups (As 50 ppm and HFD + As 50 ppm) were examined using RT2 profiler PCR arrays-mouse apoptosis (Fig. 7). In this respect, the HFD significantly increased the expression of Traf1, Atf5, Birc3, caspases 8, and Gadd45 genes and it consequently decreased the expression of Bcl2a1a, Naip2, Cidea, Aifm1, Nol3, Birc5,

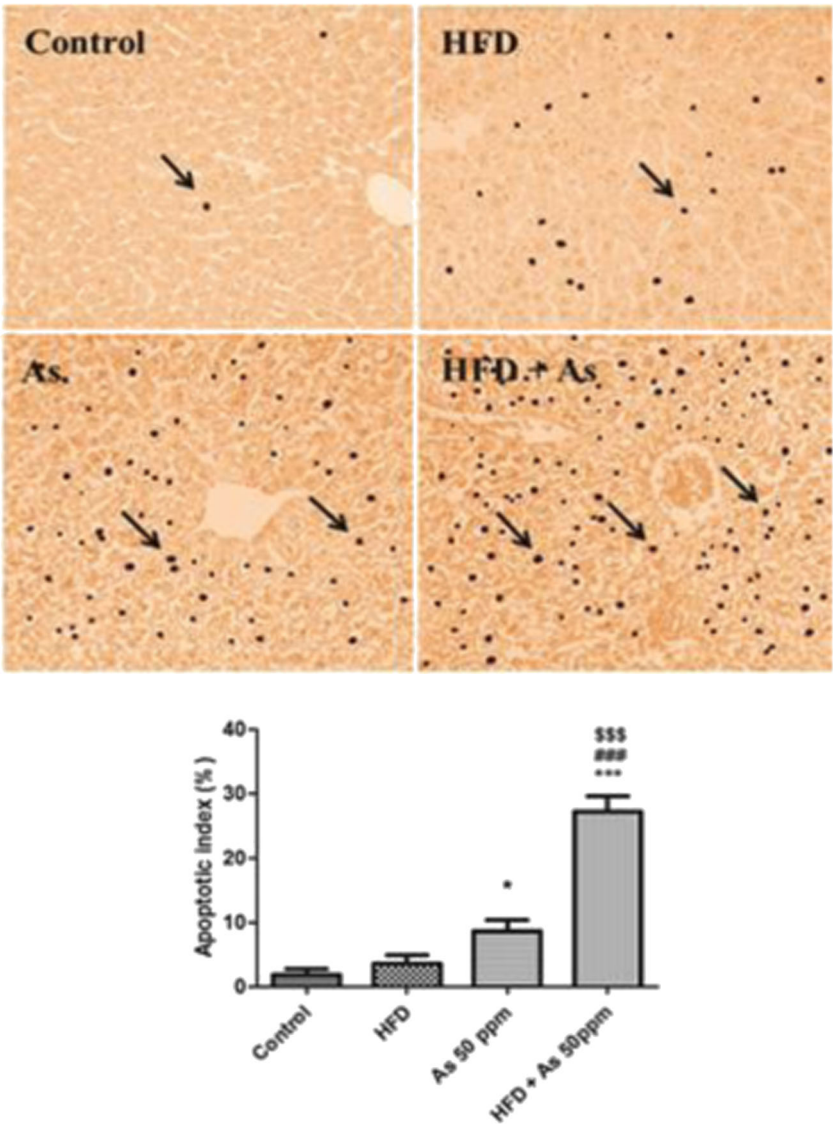

Fig. 4 Light microscopy of cross-sections of TUNEL-stained liver and apoptotic index from control group, HFD group, and As-treated groups (As 50 ppm and HFD + As 50 ppm). Magnification, × 250. Arrows indicate apoptosis (TUNEL-positive cells). Values represented as mean ± SEM (n = 10). Asterisks mean significantly different from control. Number signs mean significantly different from HFD. Dollar signs mean significantly different from As. * $p < 0.05$; ***, ###, and $$$ $p < 0.001$

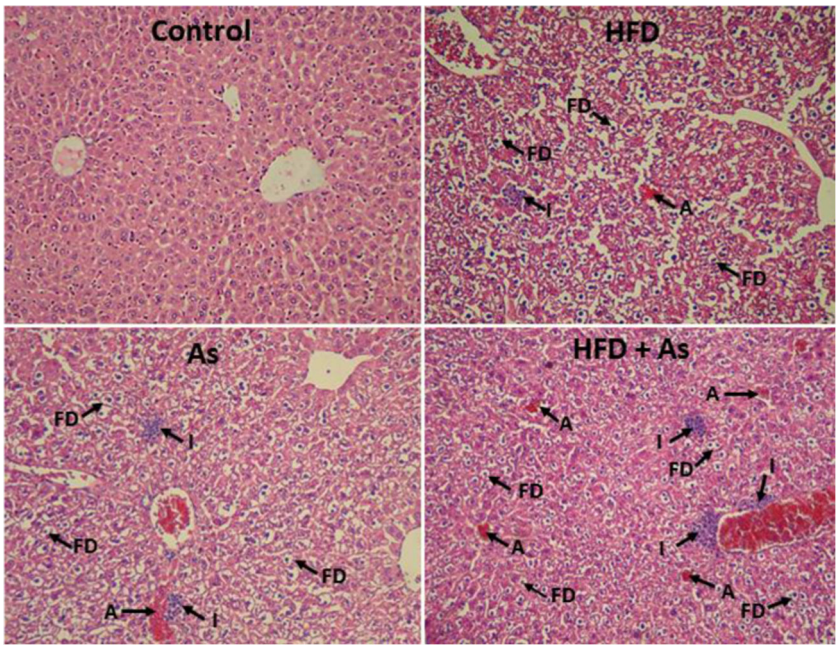

Fig. 5 Histopathological findings of liver sections stained with H&E under light microscope. Magnification, ×400. Control group, HFD group, As-treated group (As 50 ppm and HFD + As 50 ppm). Arrow A accumulation of RBCs, Arrow I infiltration of inflammatory cells, Arrow FD fat deposit

Cflar, caspase12, Bcl2l10, Trp73, Lhx4, Il10, Abl1, Trp63, and Cd70 ones in the livers of the given mice (Figs. 8 and 11). Moreover, several genes of apoptosis-related indicators were multiplied in the liver tissues of the As group compared with that in the control group (Caspase14, Cd40, Abl1, Trp63, Traf1, Bcl2l10, Cd70, Trp73, Lhx4, Il10, Cidea, Cd40lg, Polb, Fasl, TNF, Traf2, Caspase 8, Bad, and BCL-2); in contrast, the expression of Cflar, Apaf1, Ripk1, Tnfrsf11b, Naip2, Birc5, Birc3, and caspases 3 genes decreased (Figs. 9 and 11). Considering the HFD + As group, the study results showed the increased expression of caspase 8 genes and the decreased expression of Bcl2a1a, Cideb, Tnfrsf10b, Polb, Pycard, Tnfrsf11b, Naip2, Birc5, Tnfrsf1a, Igf1r, Caspase1, Bcl10, Caspase4, Apaf1, Cd40lg, Bok, Fasl, caspases 3, and caspases 12 ones (Fig. 10 and 11).

Cytochrome C release

Cytochrome C is a multi-functional enzyme involved in life and death decisions of the cells. The release of cytochrome C is thus accompanied by a sharp increase in ROS production that is essential for the formation of the apoptosome and the progression of apoptosis (Hüttemann et al. 2011). In this study, the amount of cytochrome C release significantly

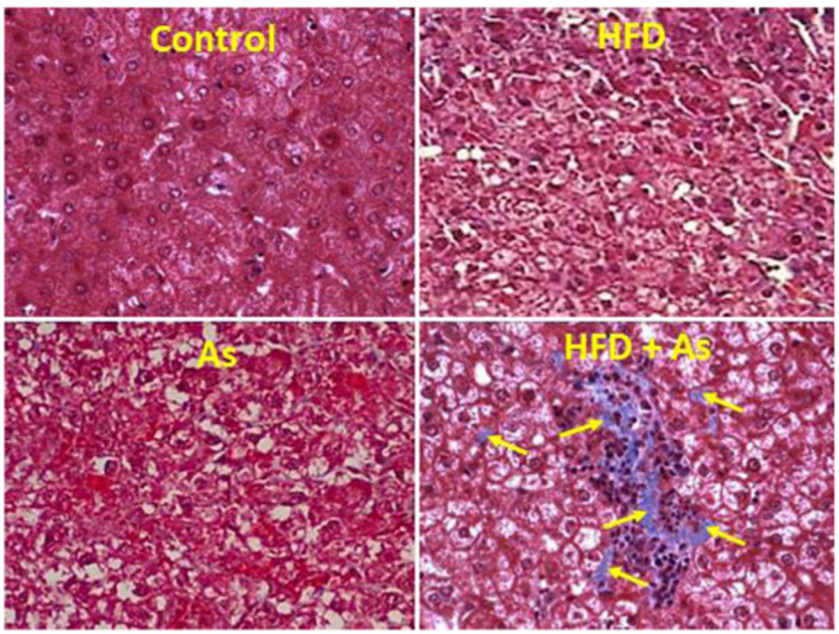

Fig. 6 Light microscopy of liver tissue stained with trichrome in various groups. Magnification, ×400. Arrows indicate fibrosis

Table 4 Semi quantitative scoring of damage on histopathological examination of liver in control group, HFD group, and As-treated groups (As 50 ppm and HFD + As 50 ppm)

Histological criteria	Groups			
	Control	HFD	As 50 ppm	HFD + As 50 ppm
Accumulation of RBC	0.09 ± 0.00	1.42 ± 0.33**	1.55 ± 0.28**	2.36 ± 0.41$^{***\#\#\$\$}$
Infiltration of inflammatory cells	0.04 ± 0.00	0.93 ± 0.56***	1.21 ± 0.00***	2.85 ± 0.38$^{***\#\#\$}$
Fibrosis	0.00 ± 0.0	0.00 ± 0.00	0.00 ± 0.00	2.12 ± 0.75$^{***\#\#\#\$\$\$}$
Fat deposit (%)	0.01 ± 0.00	10.7 ± 2.45***	8.09 ± 2.08***	11.6 ± 2.8$^{***\$}$

Values represented as mean ± SEM (n = 10)

* Significantly different from control

$^{\#}$ Significantly different from HFD

$^{\$}$ Significantly different from As

$^{\$}p < 0.05$, **, ##, and $\$\$p < 0.01$, ***, ###, and $\$\$\$p < 0.001$

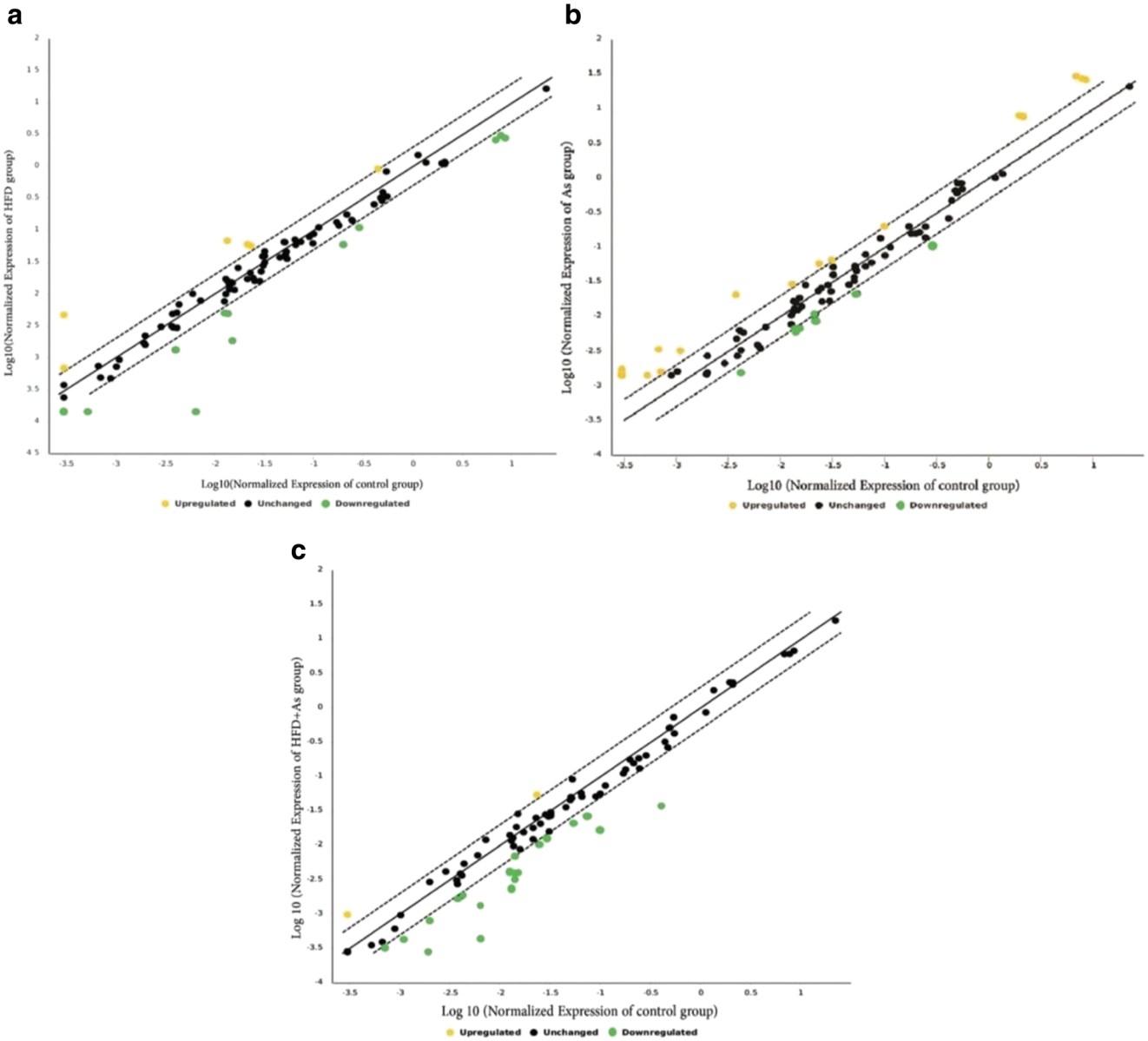

Fig. 7 The scatter plot compares the expression level ($2^{-\Delta CT}$) of each gene on the array between the control group versus the HFD group (**a**) and As-treated groups (As 50 ppm and HFD + As 50 ppm) (**b**, **c**). The black lines indicate fold changes ($2^{-\Delta\Delta CT}$) of 1. Data points beyond the dotted lines in the upper left and lower right sections meet the selected fold regulation threshold

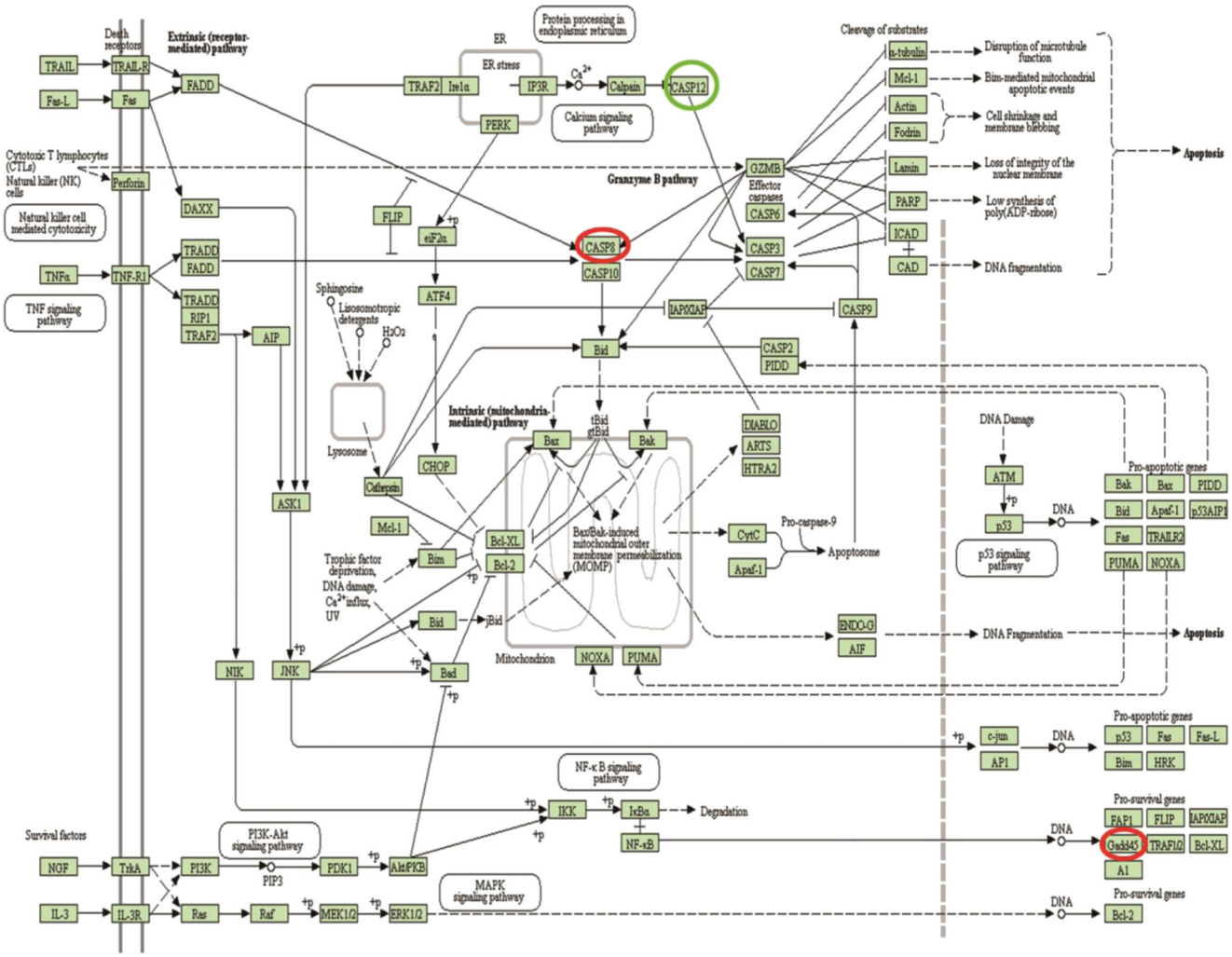

Fig. 8 KEGG pathway of differentially apoptotic hepatic gene expression and pathways. Changes in expression of apoptosis genes in HFD group (the upregulated genes are indicated by red circles and the downregulated genes are indicated by green circles)

increased after exposure to As (50 ppm) alone ($p < 0.01$) and in combination with HFD ($p < 0.001$) compared with that in the control group (Fig. 12).

Discussion

Apoptosis is known as an organized genetic pathway to maintain homeostasis in multicellular organisms (Elmore 2007). The impaired regulation of apoptosis (increase/decrease) also results in irreversible damage to cells and nearly half of human diseases. Hence, identification of apoptosis genes as well as their products and mechanisms of action is the basis for discovering new drugs to target apoptosis (Dlamini et al. 2004; Pfeffer and Singh 2018). In this respect, an increase in apoptotic activity has been observed in various liver diseases (viral hepatitis, autoimmune hepatitis, toxic damage, and fatty liver). In contrast, the decrease of apoptosis can be observed during regenerative liver growth or in liver tumors (Eichhorst 2005; Luedde et al. 2014). Thus, it is clear that apoptosis plays a crucial role in the pathogenicity of liver disease. In terms of hepatic toxicity, several toxins can cause damage to hepatocytes through the process of apoptosis, which is associated with the accumulation of Ca^{2+} in cytosol or mitochondria, ROS accumulation, and membrane damage (Guicciardi et al. 2013). With regard to high levels of cytochrome P450 in the liver, As-induced lipid peroxidation by high levels of ROS can also lead to destruction of the mitochondrial membrane. It should be noted that mitochondria as a vital source of ROS are the main targets of As-induced genotoxic responses, which are confirmed via decreasing ATP levels. In addition, studies have shown a significant reduction in GSH along with a considerable decrease of GSH-generating enzymes (G6PD and GR) as well as scavenging ones (GST, GPx, SOD, CAT) during exposure to As (Liu et al. 2005; Pi et al. 2002; Ramanathan et al. 2002). According to the results of the present study, As could boost the production of pro-oxidants and reduce the antioxidant effect of the GSH. The SOD enzyme

activity had also significantly decreased as the first defense line against oxidative stress as well as the activity of catalase and GPx as scavenging H_2O_2 enzymes (Fig. 3, Table 3). As-induced oxidative stress was similarly considered as the most important trigger for apoptosis. Besides, As, leading to mitochondrial dysfunction, could alter BAX/BCL-2 ratio, caspase activity, and eventually apoptosis (Singh et al. 2010). Based on the study results, As could activate external apoptosis pathway through FasL receptor via increasing the expression of Caspase 8. Overall, two FasL-mediated pathways activated Caspase 8. In the first pathway, the cells directly activated high levels of Caspase 8 and subsequently Caspase 3. In the second pathway, the expression of Caspase 8 was not sufficient to activate Caspase 3, in which Caspase 8 led to cleavage and activation of BH3-only protein (Bid), release of cytochrome C from mitochondria, and induction of apoptosis (Parrish et al. 2013). After an apoptotic insult, activated caspases and the caspase-activated protein t-Bid can trigger the release of apoptosis-inducing factor (AIF) from mitochondria and AIF translocates to the cytosol and the nucleus, where it induces peripheral chromatin condensation, as well as DNA fragmentation. Conversely, AIF can trigger the release of cytochrome *c* from mitochondria. The mitochondrio-nuclear translocation of AIF is in a caspase-independent fashion and can be observed in cells in which there is no caspase activation, owing to knockout of Apaf-1, caspase-9, or caspase-3. These finding indicate that AIF can act as a caspase-independent death effector (Candé et al. 2002). The second pathway was more likely in the present research, given the increased cytochrome C release and decreased Caspase 3 expression. Investigations had also demonstrated that liver damage could be associated with apoptosis and NF-κB activation even if anti-apoptotic BCL-2 had a high expression, a finding that might justify the increase of anti-apoptotic BCL-2 in the As group in this study (Ramalho et al. 2006; Ribeiro et al. 2004). Moreover, increased expression of Trp63 as one of the tested genes in the present study induced apoptosis through death receptors and mitochondrial pathways, and it was assumed that the ability of

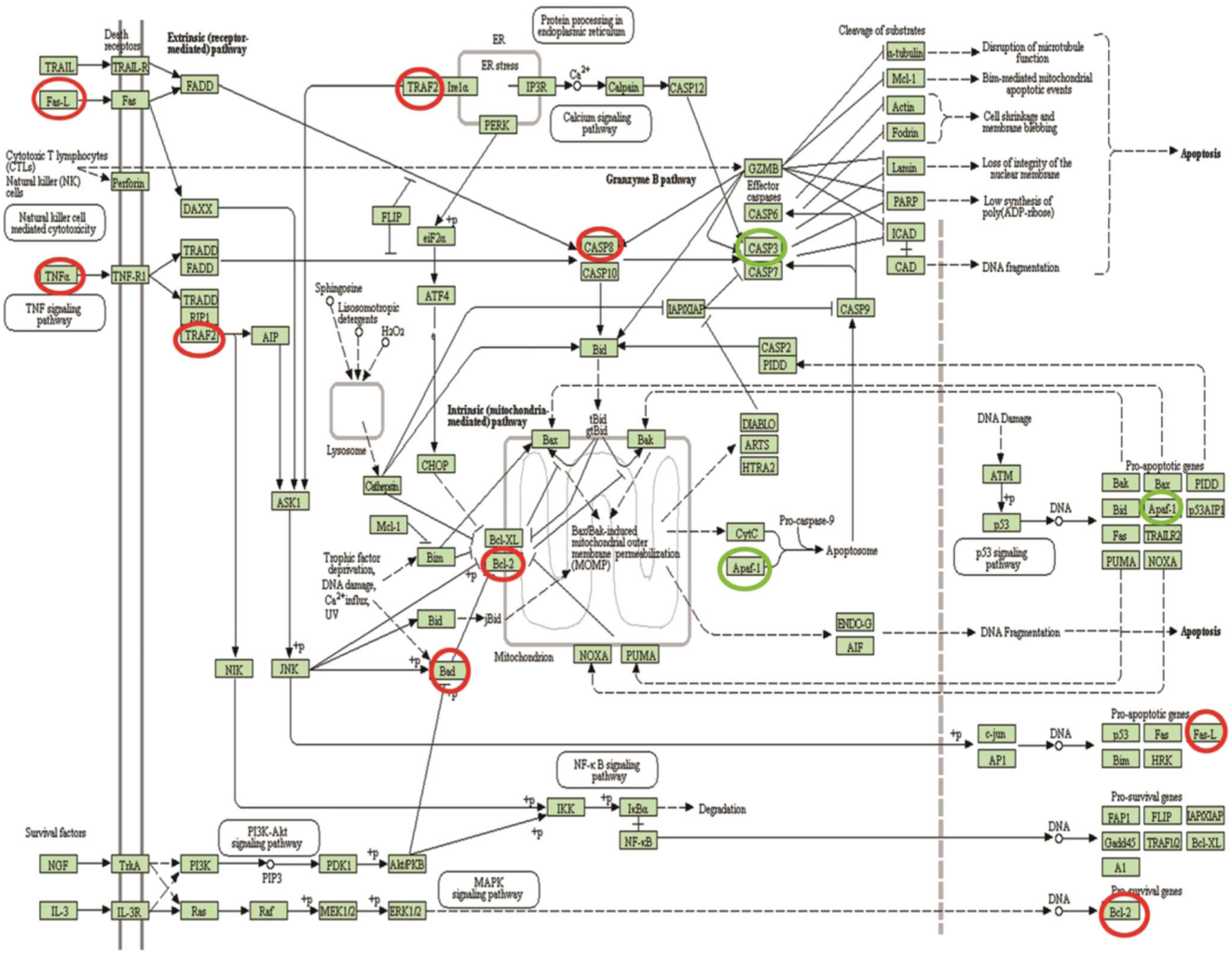

Fig. 9 KEGG pathway of differentially apoptotic hepatic gene expression and pathways. Changes in expression of apoptosis genes in As group (the upregulated genes are indicated by red circles and the downregulated genes are indicated by green circles)

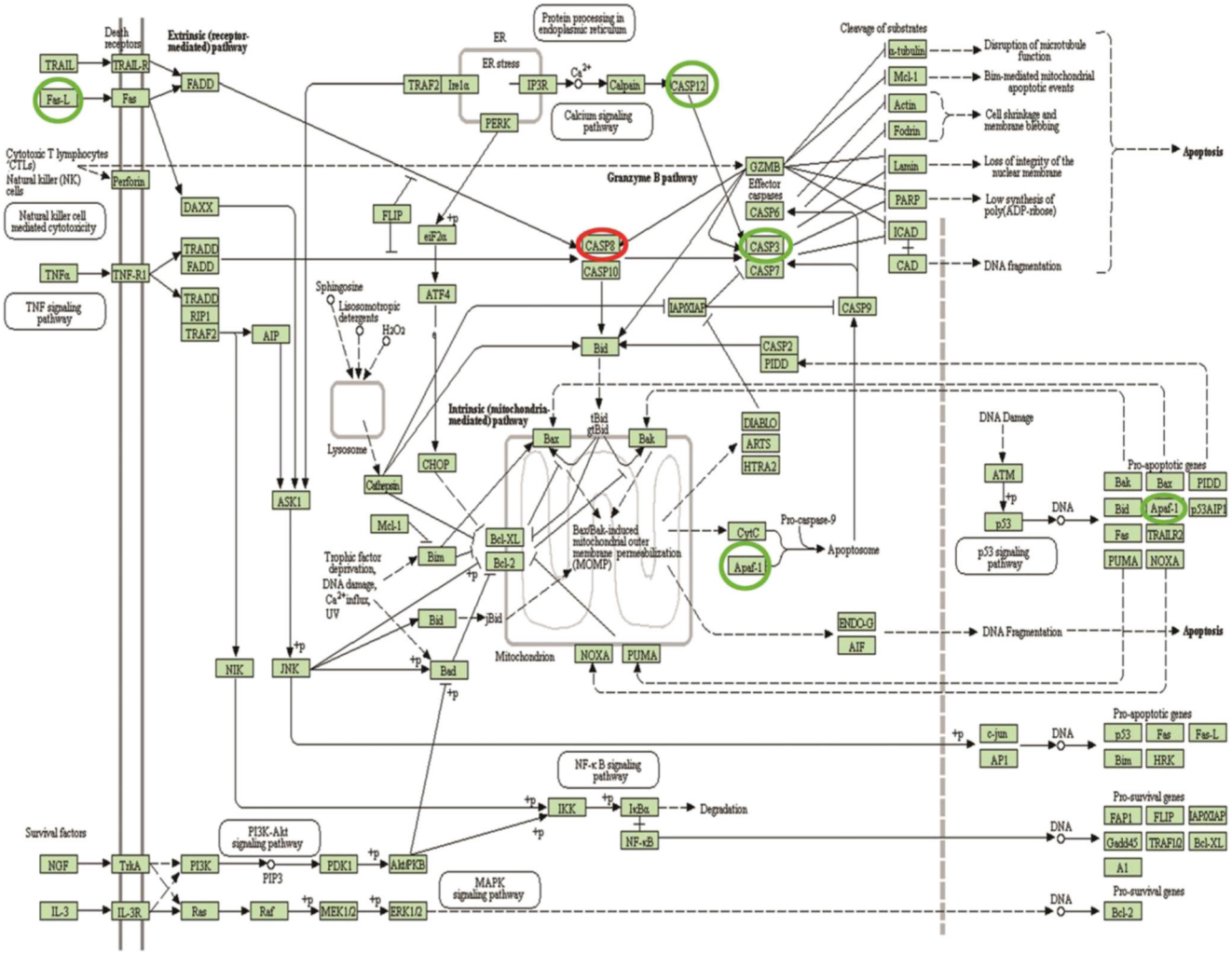

Fig. 10 KEGG pathway of differentially apoptotic hepatic gene expression and pathways. Changes in expression of apoptosis genes in As + HFD group (the upregulated genes are indicated by red circles and the downregulated genes are indicated by green circles)

p53 to induce apoptosis was dependent upon Trp63 and Trp73 (El Husseini and Hales 2017). Abll activity was also correlated with the activity of P53 and its related proteins. Accordingly, Abll gene was activated in response to ROS, oxidative stress, and DNA damage that led to induction of apoptosis and inhibition of cell growth (Sourbier et al. 2014; Wang et al. 2006), which was consistent with the results obtained in the As group in this study (Fig. 11). The results of the investigation by Derdak similarly indicated that P53 and its transcriptional targets were involved in the pathogenesis of liver diseases (Derdak et al. 2013).

The HFD also brought about mitochondrial dysfunction via decreased ATP levels, increase in oxidative stress, reduction of the content of key mitochondrial proteins (including antioxidants), and eventually development of obesity (Benard et al. 2016). Under these conditions, myocytes and adipocytes could become resistant to insulin, leading to hyperglycemia, hyperlipidemia, and ectopic accumulation of fat in liver tissues (Wang 2014). It should be noted that chronic hyperglycemia in obese individuals instigate continuous production of high MDA levels and higher production of ROS, increasing oxidative stress and impairing glucose metabolism (Figs. 2 and 3 and Table 3). Confirming impaired glucose metabolism, studies by He et al. showed that TRP73 had increased pentose phosphate pathway (PPP) and improved the synthesis of NADPH and ribosomes from G6PD, and hence, the reduction of its flow would lead to increasing glucose levels. Moreover, TRP73 expression had seriously reduced due to the high level of DNA damage, but apoptosis was not significantly induced (Chen et al. 2014; He et al. 2015). In the present study, TRP73 expression in the HFD group had significantly reduced compared with that in the control group and it confirmed the mentioned findings (Fig. 11). It should be noted that Cideb is known as one of the major genes regulating the development of obesity and diabetes via controlling the biosynthesis of fatty acids and cholesterol as well as their secretion and storage in hepatocytes which significantly decreased in the As + HFD group in this study (Fig. 11). According to the studies conducted by Li et al.,

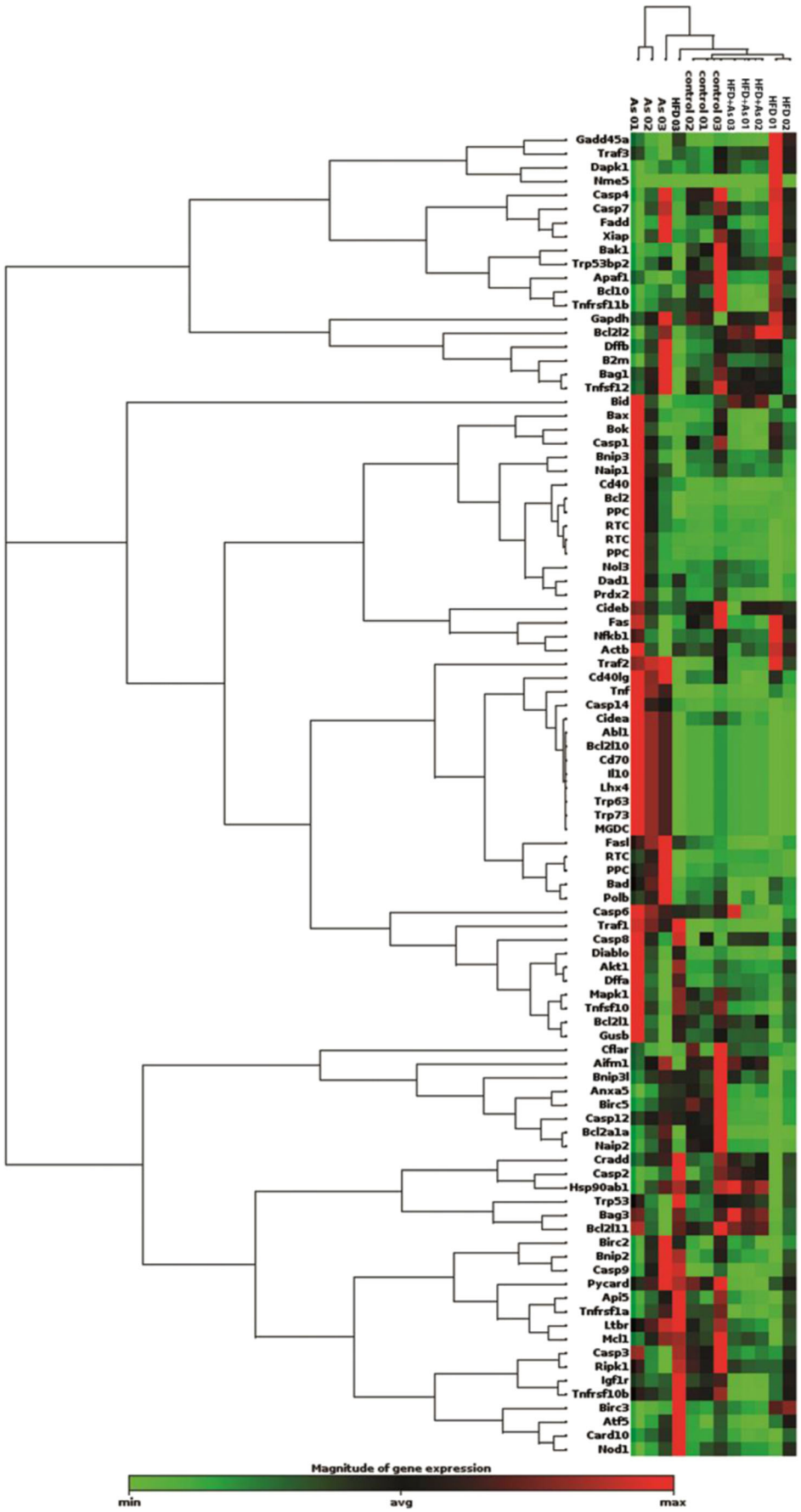

Fig. 11 The clustergram indicating co-regulated apoptosis genes across control group versus the HFD group and As-treated groups (As 50 ppm and HFD + As 50 ppm)

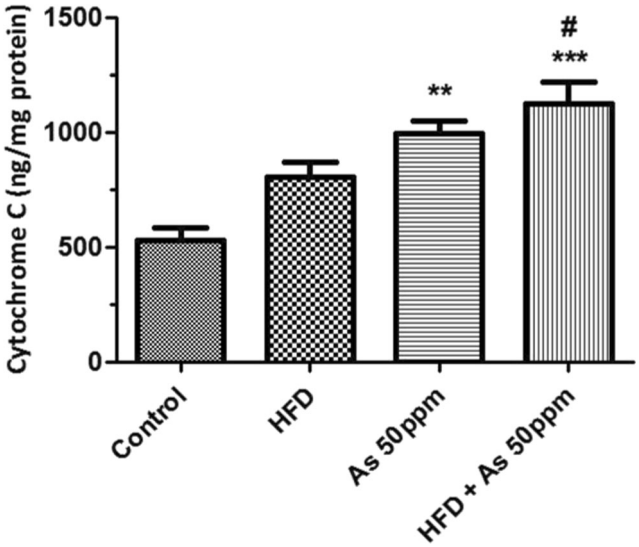

Fig. 12 Cytochrome C level in control group, HFD group, and As-treated groups (As 50 ppm and HFD + As 50 ppm). Values represented as mean ± SEM ($n = 10$). Asterisks mean significantly different from control. Number sign means significantly different from HFD. $^{\#}p < 0.05$, $^{**}p < 0.01$, $^{***}p < 0.001$

increased energy consumption, resistance to insulin, obesity, and diabetes were observed among mice deficient in TRP73 gene (Li et al. 2012). In addition, based on the research by Skeldon, reduced expression of Caspase 12 in a group of mice receiving HFD led to the development of obesity, glucose intolerance, and insulin resistance (Skeldon and Morizot 2016). These findings were in agreement with the results obtained from the HFD and HFD + As groups in terms of weight changes in mice, as well as the results of Zeinvand Lorestani et al. considering diabetes induction following HFD (Zeinvand-Lorestani et al. 2018a). Furthermore, reduced level of Polb expression in the HFD + As group compared with that in the control group in the present study implied the effect of oxidative stress on the induction of apoptosis, as it is known that cells deficient in this gene are more susceptible to DNA alkylating agents and H_2O_2 (Fig. 11) (Niimi et al. 2005). In a study conducted on a HFD mouse model, apoptosis was also evaluated using DAPI technique and TUNEL staining, and it was reported that the severity of apoptosis had increased in the livers of a group of mice under this regimen, which was a feature of liver insulin resistance due to HFD. They also suggested interactions between proteins related to insulin resistance and hepatocellular damage (caused by TNF, NF-Kβ, and JNK) as a potential risk of apoptosis in the liver (Soltis et al. 2017). In a study in 2014, it was found that apoptosis rates in rats receiving HFD with diethylnitrosamine (DEN) were higher than those reported in the control group, which predisposed hepatocellular carcinoma (HCC) to programmed cell death. Therefore, it could be stated that the mechanism of HFD treatment might delay the induction of HCC due to DEN (Duan et al. 2014). According to the results of the present study, the expression of Caspase 8 as a cysteine protease, playing a vital role in the external pathway of apoptosis signaling with cell death receptors, had increased as a result of cellular stress in all the three groups. Likewise, based on the results of cytochrome C release, pathologic studies, and TUNEL staining, it was concluded that higher oxidative damage in a combined use of As and HFD was likely to significantly intensify As-induced apoptosis in liver cells. The interesting point in this study was that the expression of Caspase 3 as a negative regulator of apoptosis in this kit had significantly reduced despite the activation of Caspase 8, suggesting that external receptors had caused events leading to apoptosis through non-Caspase 3–dependent activity.

Collectively, these data demonstrated that combined exposure to As and HFD had produced aggravating oxidative stress together with enhanced induction of hepatocytes apoptosis and an increase in the risk of liver diseases. This evidence showed that environmental toxicants such as could influence risk factors leading to hepatocellular damage. Today, the risk of liver damage from As and HFD should be much more considered due to the increasing global incidence of liver diseases as well as the willingness of communities to industrialize and consume estern foods. Besides, this hypothesis might offer a new strategy in view of the high induction of apoptosis for cancer treatment, which requires more experiments and further investigations on cancer cells considering the side effects.

Conclusion

Considering that the competitive and cooperative response of pro-apoptotic and anti-apoptotic axis always exists during chemical exposure and the causes of cellular stress, and given that any single molecule is not responsible to determine the fate of the cell, we designated the cluster of all genes involved in apoptosis following exposure to arsenic and high-fat diet in order to elucidate apoptosis pathways further. It has been concluded that the extrinsic pathway is the initial process of apoptosis and caspase 8 was activated as a cysteine protease, which plays an essential role in the external apoptosis signaling pathway with cell death receptors. While the internal pathway activation is a secondary pathway and induced apoptosis through caspase 3–independent mechanisms.

Based on these findings, we anticipate that our report will provide a novel outlook in targeting molecules for inducing apoptosis in hepatocellular carcinoma as well as inhibiting apoptosis in normal cells.

Author contributions Azin Samimi designed the experiments, analyzed the data, and prepared the manuscript. Ali Teimoori, Hadis Alidadi, and Azin Samimi performed the experiments. Heibatullah Kalantari, Mohammad Javad Khodayar, Najmaldin Saki, and Layasadt Khorsandi reviewed the manuscript.

Funding information This paper is issued from Ph.D. thesis Azin Samimi and was financially supported by Toxicology Research Center (Grant number TRC-9608) of Ahvaz Jundishapur University of Medical Sciences.

Compliance with ethical standards

Competing interests The authors declare that they have no competing interests

References

Aebi H (1984) Catalase in vitro Methods in enzymology 105:121-126

Ahangarpour A, Alboghobeish S, Rezaei M, Khodayar MJ, Oroojan AA, Zainvand M (2018) Evaluation of diabetogenic mechanism of high fat diet in combination with arsenic exposure in male mice. Iran J Pharm Res 17:164–183

Ahmed M (2015) Non-alcoholic fatty liver disease in 2015. World J Hepatol 7:1450

Bashir S, Sharma Y, Irshad M, Nag TC, Tiwari M, Kabra M, Dogra TD (2006) Arsenic induced apoptosis in rat liver following repeated 60 days exposure. Toxicology 217:63–70. https://doi.org/10.1016/j.tox.2005.08.023

Benard O, Lim J, Apontes P, Jing X, Angeletti RH, Chi Y (2016) Impact of high-fat diet on the proteome of mouse liver. J Nutr Biochem 31:10–19

Bradford MM (1976) A rapid and sensitive method for the quantitation of microgram quantities of protein utilizing the principle of protein-dye binding. Anal Biochem 72:248–254

Buege JA, Aust SD (1978) Microsomal lipid peroxidation. Methods Enzymol 52:302–310

Candé C, Cecconi F, Dessen P, Kroemer G (2002) Apoptosis-inducing factor (AIF): key to the conserved caspase-independent pathways of cell death? J Cell Sci 115(24):4727–4734

Chakraborty JB, Oakley F, Walsh MJ (2012) Mechanisms and biomarkers of apoptosis in liver disease and fibrosis Int J Hepatol 2012

Chen D, Ming L, Zou F, Peng Y, Van Houten B, Yu J, Zhang L (2014) TAp73 promotes cell survival upon genotoxic stress by inhibiting p53 activity. Oncotarget 5:8107

Choi SS, Diehl AM (2008) Hepatic triglyceride synthesis and nonalcoholic fatty liver disease. Curr Opin Lipidol 19:295–300

Choudhury S, Ghosh S, Mukherjee S, Gupta P, Bhattacharya S, Adhikary A, Chattopadhyay S (2016) Pomegranate protects against arsenic-induced p53-dependent ROS-mediated inflammation and apoptosis in liver cells. J Nutr Biochem 38:25–40

Derdak Z, Villegas KA, Harb R, Wu AM, Sousa A, Wands JR (2013) Inhibition of p53 attenuates steatosis and liver injury in a mouse model of non-alcoholic fatty liver disease. J Hepatol 58:785–791

Dlamini Z, Mbita Z, Zungu M (2004) Genealogy, expression, and molecular mechanisms in apoptosis. Pharmacol Ther 101:1–15

Doğanyiğit Z, Silici S, Demirtaş A, Kaya E, Kaymak E (2019) Determination of histological, immunohistochemical and biochemical effects of acute and chronic grayanotoxin III administration in different doses in rats. Environ Sci Pollut Res 26 (2):1323–1335

Duan X-Y, Pan Q, Yan S-Y, Ding W-J, Fan J-G, Qiao L (2014) High-saturate-fat diet delays initiation of diethylnitrosamine-induced hepatocellular carcinoma. BMC Gastroenterol 14:195

Dutta M et al (2014) High fat diet aggravates arsenic induced oxidative stress in rat heart and liver. Food Chem Toxicol 66:262–277

Eichhorst ST (2005) Modulation of apoptosis as a target for liver disease. Expert Opin Ther Targets 9:83–99

El Husseini N, Hales BF (2017) The roles of P53 and its family proteins, P63 and P73, in the DNA damage stress response in organogenesis-stage mouse embryos. Toxicol Sci 162:439–449

Ellman GL (1959) Tissue sulfhydryl groups. Arch Biochem Biophys 82:70–77

Elmore S (2007) Apoptosis: a review of programmed cell death. Toxicol Pathol 35:495–516

Elwej A, Grojja Y, Ghorbel I, Boudawara O, Jarraya R, Boudawara T, Zeghal N (2016) Barium chloride induces redox status unbalance, upregulates cytokine genes expression and confers hepatotoxicity in rats-alleviation by pomegranate peel. Environ Sci Pollut Res 23:7559-7571

Fasshauer M, Bluher M (2015) Adipokines in health and disease Trends in pharmacological sciences 36:461-470 https://doi.org/10.1016/j.tips.2015.04.014

Feldstein AE, Werneburg NW, Canbay A, Guicciardi ME, Bronk SF, Rydzewski R, Burgart LJ, Gores GJ (2004) Free fatty acids promote hepatic lipotoxicity by stimulating TNF-α expression via a lysosomal pathway. Hepatology 40:185–194

Flora SJ, Mehta A, Gupta R (2009) Prevention of arsenic-induced hepatic apoptosis by concomitant administration of garlic extracts in mice. Chem Biol Interact 177:227–233. https://doi.org/10.1016/j.cbi.2008.08.017

Guicciardi ME, Malhi H, Mott JL, Gores GJ (2013) Apoptosis and necrosis in the liver. Compr Physiol 3:977–1010

Guilherme A, Virbasius JV, Puri V, Czech MP (2008) Adipocyte dysfunctions linking obesity to insulin resistance and type 2 diabetes. Nat Rev Mol Cell Biol 9:367–377. https://doi.org/10.1038/nrm2391

He Z, Agostini M, Liu H, Melino G, Simon H-U (2015) p73 regulates basal and starvation-induced liver metabolism in vivo. Oncotarget 6:33178

Hong YS, Song KH, Chung JY (2014) Health effects of chronic arsenic exposure. Journal of preventive medicine and public health = Yebang Uihakhoe chi 47:245–252. https://doi.org/10.3961/jpmph.14.035

Hüttemann M, Pecina P, Rainbolt M, Sanderson TH, Kagan VE, Samavati L, Doan JW, Lee I (2011) The multiple functions of cytochrome c and their regulation in life and death decisions of the mammalian cell: from respiration to apoptosis. Mitochondrion 11:369–381

Jelinek D, Castillo JJ, Arora SL, Richardson LM, Garver WS (2013) A high-fat diet supplemented with fish oil improves metabolic features associated with type 2 diabetes. Nutrition 29:1159–1165

Kirsch R, Clarkson V, Shephard EG, Marais DA, Jaffer MA, Woodburne VE, Kirsch RE, Hall Pde L (2003) Rodent nutritional model of non-alcoholic steatohepatitis: species, strain and sex difference studies. J Gastroenterol Hepatol 18(11):1272–1282

Kleinert M et al (2018) Animal models of obesity and diabetes mellitus. Nat Rev Endocrinol 14:140

Li H et al (2012) Cell death-inducing DFF45-like effector b (Cideb) is present in pancreatic beta-cells and involved in palmitate induced beta-cell apoptosis. Diabetes Metab Res Rev 28:145–155. https://doi.org/10.1002/dmrr.1295

Listenberger LL, Han X, Lewis SE, Cases S, Farese RV, Ory DS, Schaffer JE (2003) Triglyceride accumulation protects against fatty acid-induced lipotoxicity Proceedings of the National Academy of Sciences 100:3077-3082

Liu J, Waalkes MP (2008) Liver is a target of arsenic carcinogenesis. Toxicol Sci 105:24–32. https://doi.org/10.1093/toxsci/kfn120

Liu S-X, Davidson MM, Tang X, Walker WF, Athar M, Ivanov V, Hei TK (2005) Mitochondrial damage mediates genotoxicity of arsenic in mammalian cells. Cancer Res 65:3236–3242

Luedde T, Kaplowitz N, Schwabe RF (2014) Cell death and cell death responses in liver disease: mechanisms and clinical relevance. Gastroenterology 147:765–783 e764

Majumdar S, Karmakar S, Maiti A, Choudhury M, Ghosh A, Das AS, Mitra C (2011) Arsenic-induced hepatic mitochondrial toxicity in rats and its amelioration by dietary phosphate. Environ Toxicol Pharmacol 31:107–118. https://doi.org/10.1016/j.etap.2010.09.011

Martinez VD, Vucic EA, Becker-Santos DD, Gil L, Lam WL (2011) Arsenic exposure and the induction of human cancers. J Toxicol 2011:1–13

Mitchell RD 3rd, Dhammi A, Wallace A, Hodgson E, Roe RM (2016) Impact of environmental chemicals on the transcriptome of primary human hepatocytes: potential for health effects. J Biochem Mol Toxicol 30:375–395. https://doi.org/10.1002/jbt.21801

Niimi N, Sugo N, Aratani Y, Koyama H (2005) Genetic interaction between DNA polymerase β and DNA-PKcs in embryogenesis and neurogenesis. Cell Death Differ 12:184

Nutt LK, Gogvadze V, Uthaisang W, Mirnikjoo B, McConkey DJ, Orrenius S (2005) Research paper indirect effects of Bax and Bak initiate the mitochondrial alterations that lead to cytochrome c release during arsenic trioxide-induced apoptosis. Cancer Biol Ther 4: 459–467

Paglia DE, Valentine WN (1967) Studies on the quantitative and qualitative characterization of erythrocyte glutathione peroxidase. J Lab Clin Med 70:158–169

Parrish AB, Freel CD, Kornbluth S (2013) Cellular mechanisms controlling caspase activation and function. Cold Spring Harb Perspect Biol 5:5. https://doi.org/10.1101/cshperspect.a008672

Pfeffer CM, Singh ATK (2018) Apoptosis: a target for anticancer therapy. Int J Mol Sci 19. https://doi.org/10.3390/ijms19020448

Pi J et al (2002) Evidence for induction of oxidative stress caused by chronic exposure of Chinese residents to arsenic contained in drinking water. Environ Health Perspect 110:331

Ramalho RM et al (2006) Apoptosis and Bcl-2 expression in the livers of patients with steatohepatitis. Eur J Gastroenterol Hepatol 18:21–29

Ramanathan K, Balakumar B, Panneerselvam C (2002) Effects of ascorbic acid and a-tocopherol on arsenic-induced oxidative stress. Hum Exp Toxicol 21:675–680

Rector RS, Thyfault JP, Uptergrove GM, Morris EM, Naples SP, Borengasser SJ, Mikus CR, Laye MJ, Laughlin MH, Booth FW, Ibdah JA (2010) Mitochondrial dysfunction precedes insulin resistance and hepatic steatosis and contributes to the natural history of non-alcoholic fatty liver disease in an obese rodent model. J Hepatol 52:727–736

Rehman K, Naranmandura H (2013) Double-edged effects of arsenic compounds: anticancer and carcinogenic effects. Curr Drug Metab 14:1029–1041

Ribeiro PS, Cortez-Pinto H, Solá S, Castro RE, Ramalho RM, Baptista A, Moura MC, Camilo ME, Rodrigues CMP (2004) Hepatocyte apoptosis, expression of death receptors, and activation of NF-κB in the liver of nonalcoholic and alcoholic steatohepatitis patients. Am J Gastroenterol 99:1708–1717

Roy S, Narzary B, Ray A, Bordoloi M (2016) Arsenic-induced instrumental genes of apoptotic signal amplification in death-survival interplay. Cell Death Dis 2:16078. https://doi.org/10.1038/cddiscovery.2016.78

Santra A, Chowdhury A, Ghatak S, Biswas A, Dhali GK (2007) Arsenic induces apoptosis in mouse liver is mitochondria dependent and is abrogated by N-acetylcysteine. Toxicol Appl Pharmacol 220:146–155

Singh AP, Goel RK, Kaur T (2011) Mechanisms pertaining to arsenic toxicity. Toxicol Int 18:87–93. https://doi.org/10.4103/0971-6580.84258

Singh S, Greene RM, Pisano MM (2010) Arsenate-induced apoptosis in murine embryonic maxillary mesenchymal cells via mitochondrial-mediated oxidative injury. Birth Defects Research Part A: Clinical and Molecular Teratology 88:25–34

Skeldon AM, Morizot A (2016) Caspase-12, but not caspase-11, inhibits obesity and insulin resistance 196:437-447 https://doi.org/10.4049/jimmunol.1501529

Soltis AR et al (2017) Hepatic dysfunction caused by consumption of a high-fat diet. Cell Rep 21:3317–3328

Sourbier C et al (2014) Targeting ABL1-mediated oxidative stress adaptation in fumarate hydratase-deficient cancer. Cancer Cell 26:840–850

Wahlang B, Beier JI, Clair HB, Bellis-Jones HJ, Falkner KC, McClain CJ, Cave MC (2013) Toxicant-associated steatohepatitis. Toxicol Pathol 41:343–360. https://doi.org/10.1177/0192623312468517

Wang B, Sun J, Ma Y, Wu G, Shi Y, Le G (2014) Increased oxidative stress and the apoptosis of regulatory T cells in obese mice but not resistant mice in response to a high-fat diet. Cell Immunol 288:39–46. https://doi.org/10.1016/j.cellimm.2014.02.003

Wang JY, Minami Y, Zhu J (2006) Abl and Cell Death. In: Abl Family Kinases in Development and Disease. Springer, pp 26-47

Wang K (2014) Molecular mechanisms of hepatic apoptosis. Cell Death Dis 5:e996. https://doi.org/10.1038/cddis.2013.499

Wang K (2015) Molecular mechanisms of hepatic apoptosis. Cell Death Dis 5:e996

Yu W-R, Baptiste DC, Liu T, Odrobina E, Stanisz GJ, Fehlings MG (2009) Molecular mechanisms of spinal cord dysfunction and cell death in the spinal hyperostotic mouse: implications for the pathophysiology of human cervical spondylotic myelopathy. Neurobiol Dis 33:149–163

Zeinvand-Lorestani M, Kalantari H, Khodayar MJ, Teimoori A, Saki N, Ahangarpour A, Rahim F (2018a) Autophagy upregulation as a possible mechanism of arsenic induced diabetes 8:11960 https://doi.org/10.1038/s41598-018-30439-0

Zeinvand-Lorestani M et al (2018b) Dysregulation of Sqstm1, mitophagy, and apoptotic genes in chronic exposure to arsenic and high-fat diet (HFD). Environ Sci Pollut Res Int 25:34351–34359. https://doi.org/10.1007/s11356-018-3349-4

Zou Y, Li J, Lu C, Wang J, Ge J, Huang Y, Zhang L, Wang Y (2006) High-fat emulsion-induced rat model of nonalcoholic steatohepatitis. Life Sci 79(11):1100–1107